NJC

Accepted Manuscript

This is an *Accepted Manuscript*, which has been through the Royal Society of Chemistry peer review process and has been accepted for publication.

Accepted Manuscripts are published online shortly after acceptance, before technical editing, formatting and proof reading. Using this free service, authors can make their results available to the community, in citable form, before we publish the edited article. We will replace this *Accepted Manuscript* with the edited and formatted *Advance Article* as soon as it is available.

You can find more information about *Accepted Manuscripts* in the Information for Authors.

Please note that technical editing may introduce minor changes to the text and/or graphics, which may alter content. The journal's standard Terms & Conditions and the Ethical guidelines still apply. In no event shall the Royal Society of Chemistry be held responsible for any errors or omissions in this *Accepted Manuscript* or any consequences arising from the use of any information it contains.

ROYAL SOCIETY OF CHEMISTRY

www.rsc.org/njc

Synthesis and Characterisation of Novel Aluminium and Gallium Precursors for Chemical Vapour Deposition

Caroline E. Knapp, Peter J. Marchand, Caragh Dyer, Ivan P. Parkin and Claire J. Carmalt*

Department of Chemistry, University College London, 20 Gordon Street, Christopher Ingold Laboratories, London, WC1H 0AJ. Email: c.j.carmalt@ucl.ac.uk

The β-ketoimine ligand [(Me)CN(H){^{i}Pr}-CHC(Me)=O] (**L_1H**) and the bis(β-ketoimine) ligands [$(CH_2)_2${N(H)C(Me)-CHC(R)=O}$_2$] (**L_2H_2**, R = Me; **L_3H_2**, R = C_6H_5) linked by ethylene bridges have been used to form aluminium and gallium complexes: [Al(L_1)Et_2] (**1**), [Ga(L_1)$_2$Cl] (**2**), [AlL_2(O^{i}Pr)] (**3**) and [GaL_3Me] (**4**). The complexes were characterised by NMR spectroscopy, mass spectroscopy, and single crystal X-ray diffraction, with the exception of **1** which was isolated as an oil. Compounds **1 – 4** have been used for the first time as single source precursors for the deposition of Al_2O_3 (**1**, **3**) and Ga_2O_3 (**2**, **4**) respectively. Thin films were deposited *via* aerosol assisted (AA)CVD with toluene as the solvent.

Introduction

Chemical vapour deposition (CVD) of group 13 metal oxide thin films have been much studied over the last decade.[1–5] In many cases particular attention has been drawn to the design of ligand systems in order to facilitate cleaner decomposition, thus reducing contamination, increasing the volatility and solubility of precursors such that the properties of the resultant films are improved. It is well known that a bulkier R group may improve solubility but will add to carbon contamination, for example, so it is important to find the right combination of attributes to best yield the desired material.

Al_2O_3 has a band gap of 8.7 eV, remains amorphous under most conditions and is thermodynamically stable; due to these favourable properties it can be used as a gate dielectric oxide[6] and also in passivating layers.[7] In initial studies CVD of Al_2O_3 was only achievable through the oxidation of aluminium halides at high temperatures (> 700 °C)[8,9] but these films were unsuitable for microelectronic application. Alkyl aluminium species have been used in the presence of an oxidising agent to produce thin films[10,11] of the oxide at temperatures as low as 400 °C however premature reactions and particulate and carbon contamination of the films results. More recently the use of

aluminium alkoxides with oxygen[12,13] has produced films at 200 – 750 °C however, these alkoxides have a tendency to oligomerize and so are not volatile (*e.g.* $[Al(O^iPr)_3]_3$, m.p. 118 °C) eliminating them from low pressure (LP)CVD and atmospheric pressure (AP)CVD.

Whilst aluminium oxide precursors are arguably harder to isolate, gallium alkoxide precursors[4,14] are well established – readily yielding thin films of Ga_2O_3, which find application as gas sensors.[15–17] There are a number of reported routes to gallium alkoxides including the metathesis reaction of $GaCl_3$ with the salt of an alcohol,[18] the reaction of alkyl gallium species with alcohols[19,20] and the reaction of gallium amides with an alcohol.[21,22] Commercially available gallium and aluminium precursors, for example $[Al(acac)_3]$ and $[Ga(acac)_3]$[23] (acac = acetylacetonate), have been investigated and films grown with and without oxygen showed high carbon contamination.[24–26]

Recent work has highlighted the use of β-ketoiminate ligands as opposed to alkoxides – the added functionality of groups attached to the nitrogen atom enabling fine tuning of the precursor properties.[5] Group 13 β-ketoiminate complexes can act as single-source precursors, still containing a direct metal-oxygen bond within a delocalised ring including O and N donor atoms. The use of the ligand has been reported to increase thermal stability and lower the melting point. Most importantly however, is the ability to 'tune' the properties of the precursor through the functionalisation of the imine group to combat the issues presented by alkoxides and β-diketonates of poor volatility properties and/or solubility.[1] This allows the precursor to be tailored to the specific CVD application. Metal β-ketoiminate precursors ranging from zinc,[27] group 13[27–29] and, albeit unstable, group II metals[31] have been reported. A number of different R groups attached to the N donor atom have been explored and are mostly alkyl groups that increase the steric demand of the ligand, and donor functionalised groups, such as a polyether, which yield multidentate ligands.[4] These β-ketoiminate, or 'SALEN' type ligands, as they are also known have been used over the decades to isolate 5 co-ordinate aluminium and gallium compounds,[32] often isolated as dimers,[32–36] which have bettered the understanding of the reactivity of these complexes[37] and been used in catalysis[36,38,39] amongst other reactivity.

Here we describe the synthesis of a range of β-ketoiminate ligands, from a bidentate β-ketoiminate with an isopropyl group, to a tetradentate bis(β-ketoiminate) with two β-ketoiminate (bidentate) fragments tethered through the N with an ethylene bridge all the way to a bulky bis(β-ketoiminate) with a phenyl group. We discuss their reactivity with various aluminium and gallium precursors and the resultant aluminium and gallium complexes are structurally characterised and used as precursors in CVD to form thin films of their respective oxides. Problems with solubility and chemical stability are still widely reported in the literature and the investigation into these

complexes as precursors sheds light on some of the trends observed on changing R group. AACVD is a solution based technique, wherein an aerosol is used to get the precursor into the 'gas phase', here, the precursors' solubility and thermal stability is key. This technique vastly extends the range of potential precursors, allowing the investigation of how changing R group can affect not just the structure, solubility of the precursor but also give extra means to control film morphology and properties of the deposited materials.[40]

Results and Discussion

Compound Synthesis: β-ketoiminates and bis(β-ketoiminates). Ligand **L_1H** ([(Me)CN(H){^{i}Pr}-CHC(Me)=O] was synthesized *via* a simple 1:1 condensation reaction of acetylacetone and isopropyl amine and isolated in high purity and good yield. Isolation of the sodium salt of **L_1** proved troublesome despite more vigorous conditions, it is thought that this could be due to the tendency of smaller compounds of this type to oligomerise, so 1.1 equivalents of KH were added in THF to isolate K**L_1** in good yield. [$(CH_2)_2${N(H)C(Me)-CHC(Me)=O}$_2$] (**L_2H_2**) and [$(CH_2)_2${N(H)C(Me)-CHC(C_6H_5)=O}$_2$] (**L_3H_2**) were synthesized in a similar manner according to the literature procedure and were isolated as crystalline solids, also in good yield.[41]

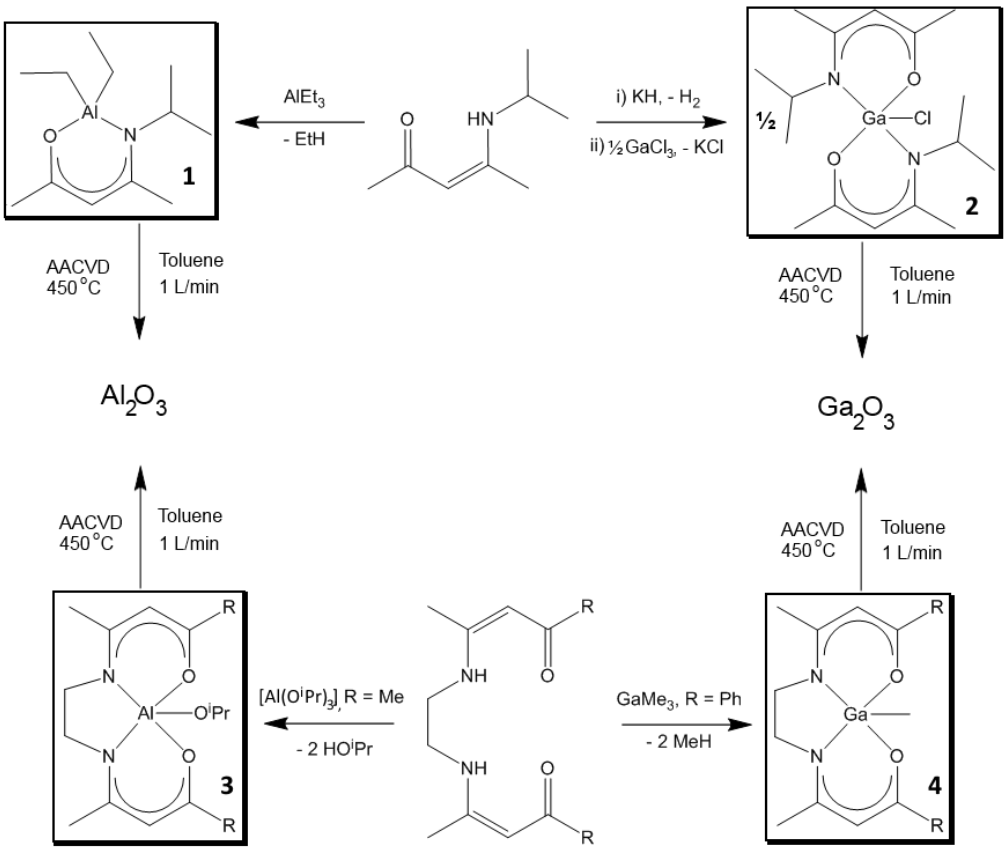

Scheme 1: Synthesis of β-ketoiminate Metal Complexes 1 – 4.

Overnight reflux of a 1:1 mixture of $AlEt_3$ with **L_1H** afforded $[Al(L_1)Et_2]$ (**1**) as a viscous yellow oil confirmed by ^1H, ^{13}C NMR, MS and EA. The proton NMR resonances to the ligand environments were significantly shifted from the free ligand, confirming coordination to the metal centre, furthermore the 2:1 ratio of ethyl groups to ligand **L_1** provides further evidence of the formation of **1**. Attempts to isolate the bis(β-ketoiminate): $[Al(L_1)_2Et]$ were unsuccessful after stirring or reflux with 1:2 and 1:8 reaction mixtures.

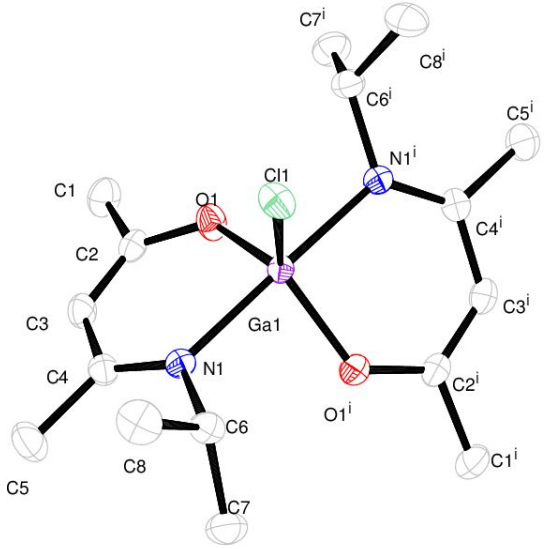

Figure 1. ORTEP diagram showing complex 2. Thermal ellipsoids are drawn at 50% probability, hydrogen atoms omitted for clarity.

A hexane suspension of two equivalents of K**L_1** with $GaCl_3$ required reflux conditions overnight to form $[Ga(L_1)_2Cl]$ (**2**). ^1H and ^{13}C NMR for **2** show similar resonances to **1** for proton environments – significantly shifted from the free ligand, indicative of the formation of **2**. Isolation of **2** was confirmed by ^1H, ^{13}C NMR, MS, EA and recrystallization of **2** afforded suitable crystals for X-ray diffraction (Fig 1, Tables 1 – 2). Compound **2** is 5 coordinate with two ligands taking up 4 spaces in gallium's coordination sphere with Cl occupying an equatorial position as expected due to its relative size and electronegativity. Compound **2** crystallised in the monoclinic space group C2/c. By calculating the τ value of 5 coordinate structures (square based pyramidal τ = 0, trigonal pyramidal τ = 1) the degree of distortion, if any, can be quantified,[42] for **2**, τ = 0.95 indicates that there is almost no distortion from ideal trigonal bipyramidal geometry.

The Ga(1)-Cl(1) bond length in **2** of 2.2460(6) Å is typical of reported bonds of this type as are the Ga(1)-N(1) and Ga(1)-O(1) bond lengths of 2.0592(4) Å and 1.8690(12) Å respectively, which compare with values of 1.862(6) Å and 2.045(7) Å for the respective bonds in the *iso*-structural compound

[Ga(N,N'-phenlenebis(3,5-di-*tert*-butylsaliclideneimine)Cl] reported previously.[43] The short N(1)-C(4) and O(1)-C(2) bond lengths (1.306(2) Å and 1.308(2) Å) are indicative of the delocalised bonding in the ligand.[43] The Cl(1)-Ga(1)-O(1) angle of 119.81(4)° is typical of this equatorial position, and is almost identical to the O(1)-Ga(1)-O(1^i) angle (120.38(8)°) as expected. In the axial position the N(1)-Ga(1)-N(1^i) angle deviates slightly from the expected 180° (177.17(7)°) due to the steric constraints of the ligand. The axial to equatorial angles are also as expected: Cl(1)-Ga(1)-N(1), 91.42(4)° and N(1)-Ga(1)-O(1), 92.69(5)°, varying slightly from the expected 90°. In reference to related trigonal bipyrimidal gallium alkoxide structures such as [$ClGa(OR)_2$], the Ga-O and Ga-N bond distances and angles within the crystal structure corroborate those observed in this compound.[44]

Table 1. Selected Bond Lengths (Å) and angles (°) for Compounds 2, 3, and 4.

	2 (M = Ga) [$ClGa(L_1)_2$]	**3** (M = Al) [(^{i}PrO)AlL_2]	**4** (M = Ga) [$MeGaL_3$]
Lengths (Å)			
M – O	1.8690(12)	1.8173(14)	1.948(2)
		1.8466(13)	1.945(2)
M – N	2.0592(14)	1.9959(16)	2.032(3)
		1.9701(15)	2.037(3)
M – C	-	-	1.961(3)
M – Cl	2.2460(6)	-	-
M - O^{i}Pr	-	1.7436(13)	-
C – O	1.308(2)	1.309(2)	1.303(4)
C – N	1.306(2)	1.299(2)	1.307(4)
Angles (°)			
O – M – O	120.38(8)	88.52(6)	81.32(9)
N – M – N	177.17(7)	81.31(6)	80.60(11)
O – M – N	92.69(5)	89.04(6)	87.59(10)
		90.62(6)	87.29(9)
		128.15(7)	143.82(10)
		167.55(7)	142.07(10)
X – M – O*	119.81(4)	114.00(7)	107.26(12)
		99.62(6)	107.80(12)
X – M – N*	91.42(4)	92.53(6)	110.13(12)
		117.22(7)	108.91(12)

** X = Cl, **2**; OiPr, **3**; Me, **4**.*

The reaction of one equivalent of $\mathbf{L_2H_2}$ with [$Al(O^iPr)_3$] at elevated temperature and stirring overnight yielded compound **3** in good yield as confirmed by ^{1}H, ^{13}C NMR, MS, EA and single crystal X-ray analysis (Fig. 2, Tables 1 – 2). Proton NMR show backbone CH resonance at 5 ppm, ethylene bridge at ca. 3.5 ppm, and Me groups at 1.5 – 2.0 ppm, the resonances of the ethylene bridge appear as separate resonances due to the ligands coordination to a metal centre, as opposed to the freely rotating free ligand where the ethylene resonances appear equivalent. The ^{1}H NMR spectrum of **3** is

consistent with the presence of one ligand environment, with the set of resonances significantly differing from the free ligand. It is often observed in compounds of this type in the absence of a suitable Lewis base, that dimerization will occur, however it would appear that this has been prevented due to the bulk of $\mathbf{L_2}$.

Compound **3** crystallised in the distorted trigonal bipyramidal orthorhombic space group Pbca, with τ = 0.66. Unsurprisingly the isopropoxide ligand sits in the equatorial position with $\mathbf{L_2}$ occupying four sites and the isopropoxide completing the coordination sphere. As a direct result of the short ethylene backbone on $\mathbf{L_2}$ we observe a bond angle for N(1)-Al(1)-N(2) of 81.31(6)°, considerably smaller than the expected 90°. The level of distortion is further evidenced in the largest bond angle at aluminium, O(2)-Al(1)-N(1) (167.55°) differing somewhat from the ideal 180°. Differences between axial and equatorial bond lengths are small with Al(1)-O(1) (1.8173(14) Å) and Al(1)-N(2) (1.9701(15) Å) only being nominally smaller than their axial equivalent Al(1)-O(2) and Al(1)-N(1) (1.8466(13) and 1.9959(16) Å, respectively). Due to the steric constraints of $\mathbf{L_2}$, the isopropoxide ligand is more tightly bound (Al(1)-O(3), 1.7436(13) Å), this is also seen in the literature with other ligands of the type OR, *c.f.* Atwood *et al.* compound [salpen(^{t}Bu)AlOSiPh$_3$] which has an Al-O bond length of 1.726(2).[43] Typical of compounds of this type the short C-O and C-N distances are indicative of delocalised bonding in the ligand (Table 1, C-O and C-N for **2 – 4**).

As mentioned there is a deviation in the axial angle from 180° in **3** (167.55(7)°), however the sum of the equatorial angles are equal to 359° as expected (O(1)-Al(1)-N(2) 128.15(7)°, O(3)-Al(1)-O(1) 114.00(7)° and O(3)-Al(1)-N(2) 117.22(7)°). Furthermore axial to equatorial angles are mostly as expected (~90°) with the exception of O(3)-Al(1)-O(2) with a larger value of 99.62(6)° and the previously mentioned N(1)-Al(1)-N(2) (81.31(6)°) owing to the steric demand of the ligand. Both bond lengths and angles are comparable to previously reported compounds of this type[5] and it has been observed that ligands of a similar motif coordinated to Al-Et form a distorted square based pyramid geometry as we see with **4**.[45,46]

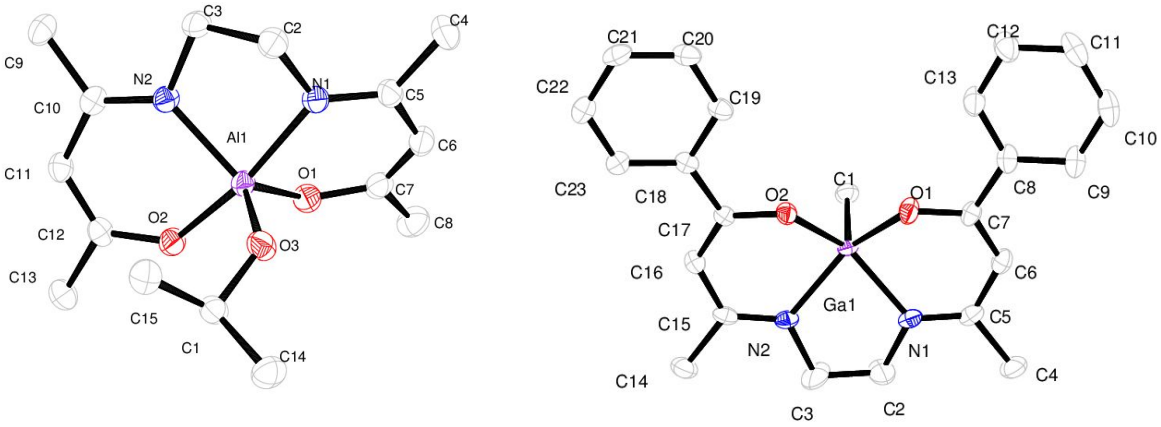

Figure 2. ORTEP diagrams showing complex 3, left, and complex 4, right. Thermal ellipsoids are drawn at 50% probability, hydrogen atoms omitted for clarity.

Refluxing one equivalent of $\mathbf{L_3}$ with $GaMe_3$ in toluene overnight afforded the crystalline product **4** in reasonable yield. Compound **4** was spectroscopically and analytically characterised using ^{1}H, ^{13}C NMR, MS, EA and single crystal X-ray analysis. As with **1 – 3** proton NMR shows significant shift from the free ligand, indicative of coordination to the metal centre, furthermore the $\mathbf{L_3}$ to Me ratio is 1:1 as expected. In the proton NMR of **4**, as with **3**, due to the inability of the ligand molecule to rotate freely there is an inequivalence of the two proton environments of the ethylene bridge.

The X-ray structure of **4** shows that $\mathbf{L_3}$ has bonded to Ga through both O atoms as expected, and the Ga centre shows a square based pyramid geometry crystallizing in the orthorhombic space group $P2_12_12_1$. In $\mathbf{L_3}$ the ethylene bridge is rigid, with one CH_2 above and another below the plane of the N and O donor atoms. A short Ga-C bond (1.961(3) Å) is indicative of a strong bond. There is no significant difference between the M-O bond distances as expected in compounds of this type, as with M-N (Table 1).

Compound **4** shows a remarkable resistance to hydrolysis compared with non-chelating aluminium alkyl species and this can be attributed in part to the high energy state of the square-based planar five coordinate Ga^{3+} species present in the molecule and also the steric bulk of the amide, since access to the nitrogen is important to the hydrolysis owing to the steric and geometric components of the mechanism of decomposition.[34,45,47] In the crystal structure of **4** the Ga is displaced from the least squares plane of the ligating nitrogen and oxygen atoms towards the methyl group and $\mathbf{L_3}$ adopts the usual inverted umbrella structure observed for monomeric transition metal species of this type. Bond angles are typical for this type of structural geometry and a selection of highlighted bond angles can be found in Table 1.

Differences are not seen in the C-O or C-N bond lengths in **4**, which are identical within error. They are also identical to the comparative lengths in compounds **2** and **3** despite the smaller ionic radius of Al^{3+} to Ga^{3+}. The high level of distortion to the trigonal bipyramidal geometry in **3** opposed to the square based pyramid geometry in **4** can be attributed jointly to the steric demands of the ligand in combination with the smaller ionic radius of Al^{3+} compared to Ga^{3+}, as well as the coordination of the smaller Me ligand in **4** as opposed to the larger O^iPr group in **3** as evidenced by the bond angles described.

Table 2. Crystallographic Data for Structurally Characterized Compounds 2 – 4.

Compound	**2** (M = Ga) [$Ga(L_1)_2Cl$]	**3** (M = Al) [$AlL_2(O^iPr)$]	**4** (M = Ga) [GaL_3Me]
Chemical formula	$C_{16}H_{28}ClGaN_2O_2$	$C_{15}H_{25}AlN_2O_3$	$C_{23}H_{25}GaN_2O_2$
Fw (g mol^{-1})	385.57	308.35	431.17
Crystal system	Monoclinic	Orthorhombic	Orthorhombic
Space group	C2/c	Pbca	$P2_12_12_1$
a (Å)	11.3771(3)	14.0647(4)	7.4044(4)
b (Å)	11.4009(3)	14.4468(4)	13.0468(6)
c (Å)	14.2678(4)	15.8435(5)	21.5066(11)
α (°)	90	90	90
β (°)	95.242(3)	90	90
γ (°)	90	90	90
V ($Å^3$)	1842.93(9)	3219.23(15)	2077.61(18)
Z	4	8	4
ρ_{calcd} (g cm^{-3})	1.390	1.272	1.378
μ (mm^{-1})	1.646	1.203	1.345
reflns collected	14260	6469	9421
unique reflns	2360	3143	4574
R_{int}	0.0504	0.0300	0.0325
R_1 and wR_2 [I > 2σ(I)]	0.0298, 0.0703	0.0391, 0.0902	0.0327, 0.0695
R_1 and wR_2 [all data]	0.0346, 0.0734	0.0568, 0.0988	0.0364, 0.0713

AACVD of 1 – 4

In order to study the feasibility of using compounds **1** – **4** as CVD precursors preliminary AACVD depositions were investigated. Anticipating that the use of the bidentate β-ketoiminate ligand may result in less carbon contamination in the films compound **1** was used initially as a precursor to thin films of Al_2O_3. AACVD of **1** in toluene afforded the best films at 450 °C on glass substrates with a 1 $Lmin^{-1}$ flow rate of nitrogen carrier gas. Films grown showed good coverage, were transparent and adhered to the substrate – passing the Scotch tape test, but could be scratched with a steel stylus. Films were also deposited on quartz but were removed upon annealing (1000 °C) which is indicative of very thin films-studies detailing the effects of delamination, wrinkling and fracture have been reported previously.[48,49] All films were resistant to a range of solvents but were easily removed using acid. X-ray diffraction (XRD) showed the films to be amorphous, as expected for films of Al_2O_3 grown at this temperature.[10,13] EDX analysis of the as deposited films confirmed the presence of aluminium, however breakthrough to the underlying silica meant that a reliable metal to oxygen ratio could not be obtained, carbon contamination was high at ~ 10 %, however it is difficult to get accurate carbon contamination levels using the techniques reported here. Filmetrics measurements calculated the films to be ~ 240 nm in thickness. SEM images of the films showed them to be smooth and relatively featureless, which is expected of thin films, however some areas revealed spherical globules (Fig. 3) it has been seen previously that thin films of Al_2O_3 are smooth with RMS roughness reported as below 1.0 nm in the literature[50] and EDX point analysis of these features confirmed the presence of aluminium.[11,12]

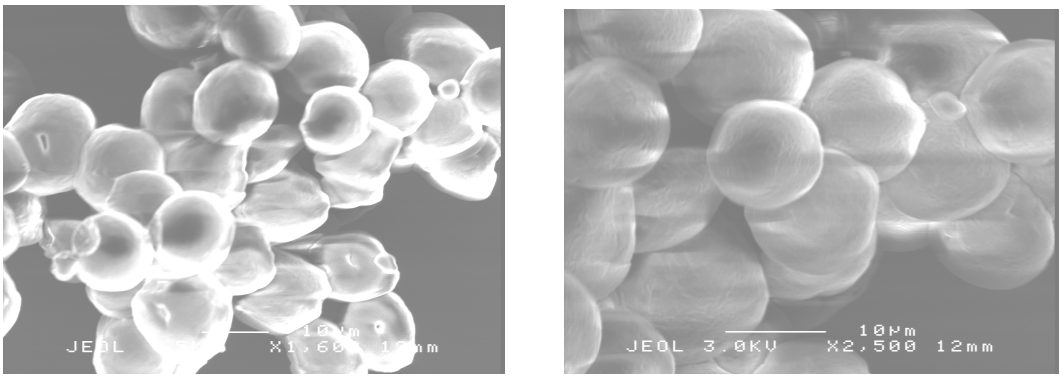

Figure 3: SEM images of the films of Al_2O_3 deposited *via* AACVD from a toluene solution of 1 on glass at 450 °C with a 1 $Lmin^{-1}$ flow rate of N_2 carrier gas.

Thin films of Al_2O_3 were grown *via* AACVD of **3** in toluene which resulted in deposition over smaller areas (*ca*. 5 cm^2) which adhered to the substrate and could only be removed using acid or a steel stylus. XRD confirmed films were amorphous. SEM revealed that the films were smooth and

featureless and concurrent EDX analysis confirmed the presence of Al in the films, as well as carbon contamination (18 %).

Despite the poorer performance of the bulkier aluminium complex, **3**, compound **1** produced conformal films and this is the first time to our knowledge that thin films of Al_2O_3 have been deposited *via* AACVD.

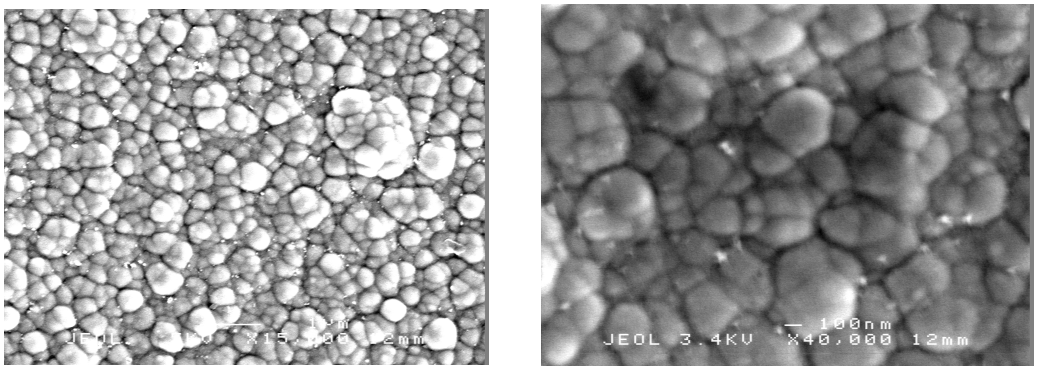

Figure 4: SEM images of the films of Ga_2O_3 deposited *via* AACVD from a toluene solution of 2, left, and 4, right, on glass at 450 °C. In both cases a 1 $Lmin^{-1}$ flow rate of N_2 carrier gas was used.

Solutions of **2** and **4** in toluene, were used in AACVD to produce thin films of Ga_2O_3. In both cases the best films were achieved at 450 °C on glass substrates with a 1 $Lmin^{-1}$ flow rate of nitrogen carrier gas. Films grown showed excellent coverage, were transparent and adhered to the substrate. UV/Vis analysis showed the films have > 80 % transparency in the visible. Using the Swanepoel method[51] the thickness of films deposited from **3** and **4** were in the range 350 – 400 nm. EDX analysis of the as deposited films confirmed the presence of gallium and carbon contamination (5 %). Films were of a sufficient thickness such that no breakthrough to the underlying substrate was observed and a metal to oxygen ratio could be calculated. For films deposited from **2** a ratio of 1:1.5, as expected was seen, films grown from compound **4** had a slightly higher oxygen content, giving a ratio of 1:1.77. It is likely in this latter case that films were not as thick and so some underlying silica was detected. SEM images of the films formed from **2** and **4** showed them to be particulate, indicative of an island growth mechanism and amorphous as expected. Carbon contamination in the films was observed however no chlorine contamination was observed in films produced from compound **2**.

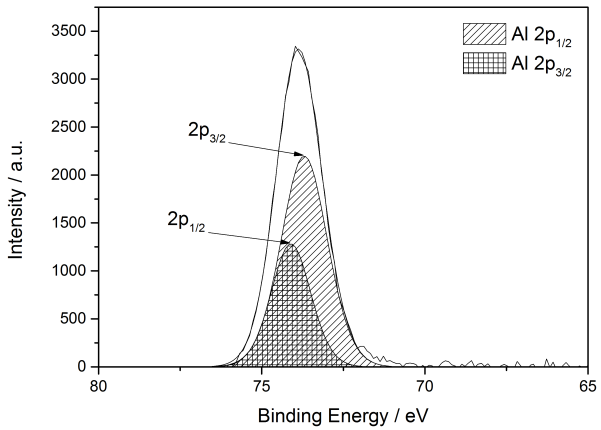

Figure 5: XPS spectrum of the Al 2p peaks from the surface of a film of Al_2O_3 deposited *via* AACVD.

X-ray photoelectron spectroscopy (XPS) was performed on samples deposited at 450 °C, pre-anneal to confirm the formation of Al_2O_3 (Figure 5). XPS confirmed the presence of aluminium and oxygen, peaks were fitted by a Gaussian/Lorentzian product distribution. As expected the binding energy of Al $2p_{3/2}$ was 73.7 eV and the Al $2p_{1/2}$ was 74.1 eV as previously reported for Al_2O_3.[52,53]

Conclusions

The isolation of monomeric group 13 precursors that do not oligermerize, with pre-formed M-O bonds has been achieved following the facile synthesis of a range of β-ketoimine ligands, furthermore compounds are readily soluble, thermally stable and decompose to their respective oxides under CVD conditions as desired. It has been shown that ligand design can significantly alter the geometry about the metal centre and the decomposition properties of the precursors as desired. The use of bidentate β-ketoiminate ligand [(Me)CN{^{i}Pr}-CHC(Me)=O] (**L_1**) isolated a bis(β-ketoiminate) gallium complex (**2**) in a trigonal bipyramidal geometry, whereas the use of the multidentate β-ketoiminate ligand: [$(CH_2)_2${NC(Me)-CHC(Me)=O}$_2$], (**L_2**) yielded the distorted trigonal bipyramidal aluminium centre, which is coordinated to one multidentate ligand and one isopropoxide group (**3**). Finally use of a sterically strained bulky ligand: [$(CH_2)_2${NC(Me)-CHC(C_6H_5)=O}$_2$], (**L_3**) coordinated to the gallium centre was isolated as a square based pyramid (**4**).

Compounds **1 – 4** have been successfully used to deposit thin films of their respective oxides on glass *via* AACVD. The aluminium β-ketoiminate compounds (**1**) and the gallium bis(β-ketoiminate) (**2**) proved to be the superior precursors affording transparent films with good coverage of Al_2O_3 and Ga_2O_3 respectively, this being the first instance that Al_2O_3 films have been deposited *via* AACVD. Extension of this work with Al_2O_3 is currently in progress.

Experimental

General Procedures.

All reactions were carried out under N_2 obtained from BOC using standard Schlenk techniques. All Solvents were dried over activated alumina by the Grubbs method using anhydrous engineering equipment, such that the water concentration was 5 – 10 ppm.[54] $GaMe_3$ was procured from SAFC Hitech, **L_1H**, **L_2H_2** and **L_3H_2** were synthesized according to literature procedures, all other starting materials were purchased from Sigma Aldrich and used without further purification. ^1H and $^{13}C\{^1H\}$ NMR spectra were obtained on a Bruker AV- 600 Mz spectrometer, operating at 295 K and 600.13 MHz (^1H). Signals are reported relative to $SiMe_4$ (δ = 0.00 ppm) and the following abbreviations are used s (singlet), d (doublet), t (triplet), q (quartet), m (multiplet), b (broad). $CDCl_3$ was obtained from GOSS Scientific and was dried and degassed over 3Å molecular sieves. Mass spectra were obtained using a Micromass 70-SE spectrometer using chemical ionization (CI) with methane reagent gas. The expected pattern for each [M]+ reported was observed. Elemental analyses were obtained at UCL.

Caution: It should be noted that $GaMe_3$ is a pyrophoric substances, which will ignite spontaneously in air and the CVD of these chemicals can potentially be toxic and corrosive. All experimental should be conducted in a fume hood. Following the deposition films are air and moisture stable and are safe to handle as any reactive species leave *via* the reactor exhaust during the AACVD process.

Synthesis.

[Al(L_2)Et_2] (1) A solution of **L_1** (1.00 g, 7.0 mmol) in toluene (20 mL) was added dropwise to a solution of $AlEt_3$ (1.62 g, 7.0 mmol) in toluene (20 mL) at -78 °C. This was stirred overnight and the solvent was removed *in vacuo* to yield a viscous yellow oily product **1** (89 %). ^1H NMR δ /ppm (C_6D_6): 4.66 (s, 1H, COCH), 3.40 (m, 1H, $CH(CH_3)_2$), 1.73 (s, 3H, CH_3CO), 1.45 (s, 3H, $CNCH_3$), 1.34 (6H, t, J = 8.12 Hz, $AlCH_2CH_3$), 1.05 (6H, d, $NCH(CH_3)_2$), 0.21 (4H, m, $AlCH_2CH_3$). $^{13}C\{^1H\}$ NMR δ /ppm 179.1 (CO), 160.6 (CN), 95.1 (CH), 44.3 ($NC(CH_3)_2$), 25.0 ($OCCH_3$), 22.5 ($NC(CH_3)_2$), 18.1 ($COCH_3$), 9.5 ($AlCH_2$), 1.3 ($AlCH_2CH_3$). M/S: m/z [ES]+ 225.0596. Elemental anal. Calc.%: C: 63.97, H: 10.74, N: 6.22, found %: C: 64.50, H: 11.12, N: 5.99.

[Ga(L_1)$_2$Cl] (2) The potassium salt of **L_1** was synthesised by adding THF (30 mL) to KH (0.852 g, 0.02 mol) and adding the resultant suspension to the **L_1H** (3 g, 0.0212 mol). The mixture was refluxed overnight and the solvent was removed in vacuo leaving a beige solid (70% yield). K**L_1** (0.5 g, 2.788 mmol) in toluene (20 mL) was added dropwise to $GaCl_3$ (0.24 g, 1.39 mmol) in toluene (20 mL) with stirring. The pale orange mixture was refluxed overnight leaving a dark brown, opaque liquid. The solvent was removed *in vacuo* leaving a brown and orange solid product. This was extracted in THF, filtered and reduced yielding **2** (78 %). Single crystals suitable for X-ray analysis were grown from

THF in the freezer for 1 week. ^{1}H NMR δ /ppm ($CDCl_3$): 5.08 (s, 1H, $(CH_3)CCH$), 4.10 (m, 1H, $(CH_3)_2CH$), 2.15 (s, 3H, CH_3CCH), 5.13 (d, 6H, J = 5 Hz, $NCHCH_3$). $^{13}C\{^{1}H\}$ NMR δ /ppm 194.7 (CO), 182.1 (CN), 99.7 ($NC(CH_3)_2$), 52.0 (CH), 29.0 ($OCCH_3$), 23.5 ($NC(CH_3)_2$), 18.8 ($OCCH_3$). M/S: m/z [ES]+ 385.1096. Elemental anal. Calc.%: C: 49.84, H: 7.32, N: 7.27, found %: C: 49.92, H: 7.56, N: 7.44.

[Al(L_2)(O^iPr)] (3) L_2H_2 (0.45 g, 2.0 mmol) was dissolved in toluene (10 mL) and added slowly *via* cannula to stirring solution of [Al(O^iPr)$_3$] (0.41 g, 2 mmol) in toluene (10 mL). The mixture was heated to 100 °C and allowed to stir for 4 hours, before being cooled slowly to room temperature and stirred for an additional 16 hours. Toluene was removed from the mixture under reduced pressure affording a yellow solid crude product. The crude product was redissolved in minimal toluene (*ca.* 5 mL) and cooled to -20 °C, affording pale yellow crystals. ^{1}H NMR δ /ppm ($CDCl_3$): 5.09 (2H, s, CH), 3.79 (1H, m, OCH), 3.62-3.65 and 3.40-3.43 (each 2H, m, CH_2), 2.01 (6H, s, $CNCH_3$), 1.97 (6H, s, $COCH_3$), 1.00 (6H, d, J = 6.12 Hz, $CH(CH_3)_2$). $^{13}C\{1H\}$ NMR δ /ppm: 180.0 (CO), 172.3 (CN), 129.1 (CH), 100.1 (CH, OCH), 62.6 (CH_2), 46.2 (CH_2), 27.6 (CH_3, $OCHCH_3$), 26.0 ($COCH_3$), 21.6 (CH_3, $CNCH_3$). M/S: m/z [ES]+ 308.35. Elemental anal. Calc.%: C: 58.43, H: 8.17, N: 9.09, found %: C: 59.01, H: 8.55, N: 9.24.

[Ga(L_3)Me] (4) A solution of L_3H_2 (1 g, 2.9 mmol) in toluene was added dropwise to solution of $GaMe_3$ (0.3 g, 2.9 mmol) at – 78 °C with stirring. This was heated to reflux and left overnight. Toluene was removed *in vacuo* affording a pale yellow product. The product was recrystallized in toluene yielding **4** (72 %). Crystals of **4** were grown from *ca*. 5 mL of toluene and were used for single crystal X-ray analysis. ^{1}H NMR δ /ppm ($CDCl_3$): 7.12-7.01 (10H, m, Ar), 5.02 (2H, s, CH), 2.92 and 2.81 (each 2H, m, CH_2), 1.91 (6H, s, $CNCH_3$), 0.18 (3H, s, $GaCH_3$). $^{13}C\{1H\}$ NMR δ /ppm: 130.0-128.3 (CH, Ar), 185.1 (CO), 172.5 (CN), 97.2 (CH), 45.7 (CH_2), 21.5 (CH_3, $CNCH_3$) 14.9 (CH_3, $GaCH_3$). M/S: m/z [ES]+ 431.09, 346.02. Elemental anal. Calc.%: C: 64.07, H: 5.84, N: 6.50, found %: C: 64.30, H: 5.92, N: 6.39.

Crystallography.

A summary of the crystal data, data collection, and refinement for crystallographically characterized compounds are given in table 2. Suitable crystals were selected and mounted on a nylon loop, the datasets of **2** - **4** were collected on a on *a SuperNova, Dual*, *Cu*, *Atlas* diffractometer. The crystal was kept at 150 K during data collection**.** Compounds **2** - **4** were solved using Olex2,[55] the structure was solved with the olex2.solve[56] structure solution program using Charge Flipping and refined with the ShelXL[57] refinement package using Least Squares minimisation. Deposit numbers for each compound: **2**: CCDC 1050516, **3**: CCDC 1050517, **4**: CCDC 1050091.

AACVD.

Depositions were carried out under dinitrogen (99.99% from BOC). Precursors were placed in an AACVD glass bubbler and an aerosol mist was created using a piezoelectric device. The solvent mist was transported in a flow of cold nitrogen from the bubbler in an 8 mm gauge pipe to a horizontal bed, cold-wall reactor (internal dimensions 15 cm × 5 cm) fitted with a graphite block containing a Whatman cartridge heater, used to heat the glass substrate. The temperature of the substrate was monitored by a Pt-Rh thermocouple. Depositions were carried out by heating the horizontal bed reactor to the required temperature before diverting the nitrogen line through the aerosol and to the reactor. The glass substrate was SiO_2, precoated (*ca.* 50 nm thick SiO_2 barrier layer) standard float glass (Pilkington NSG) 15 cm × 4 cm × 0.3 cm. A sheet of polished quartz (4 cm × 1.5 cm × 0.1 cm) was placed on the substrate 2 cm from the front of the reactor to enable a subsequent annealing step at 1000 ˚C. The substrates were cleaned prior to use, to remove surface grease. Two-way taps were used to divert the nitrogen carrier gas through the bubbler and the aerosol was carried into the reactor in a stream of nitrogen gas through a brass baffle to obtain a laminar flow. The total time for the deposition process was in the region of 30 – 90 minutes. At the end of the deposition the nitrogen flow through the aerosol was diverted and only nitrogen passed over the substrate. The glass substrate was allowed to cool with the graphite block to less than 100 ˚C before it was removed. Coated substrates were handled and stored in air. Large pieces of glass (*ca*. 4 cm × 2 cm) were used for X-ray powder diffraction. The coated glass substrate was cut into *ca.* 1 cm × 1 cm squares for subsequent analysis by scanning electron microscopy (SEM) and energy dispersive analysis of X-rays (EDX).

AACVD reactions of 1 – 4. A large number of AACVD runs were performed in order to perfect the deposition of the metal oxides. Flow rate was initially experimented with and optimised at 1 $Lmin^{-1}$, in addition a range of temperatures (350 – 550 °C) were attempted for the deposition process. Deposition times for each experiment were 60 minutes. After deposition, the bubbler was closed and the substrate allowed to cool under a flow of nitrogen. When quartz was used in the deposition process, this was added on top of the substrate before the deposition process, these were annealed for 24 hours at 1000 ˚C.

Physical Measurements.

Powder X-ray diffraction (XRD) patterns were measured on a micro-focus Bruker GADDS diffractometer equipped with monochromated Cu Kα1 radiation (Kα1 = 1.5406 Å). The diffractometer used glancing incident radiation (1.5˚). EDAX was obtained on a Philips XL30ESEM instrument, and SEM on a JEOL 6301 instrument. UV-vis-NIR spectra were recorded in the range 190-1100 nm using a Helios double beam instrument. Reflectance and transmission spectra were

recorded between 300 nm and 2300 nm by a Zeiss miniature spectrometer. Reflectance measurements were standardized relative to a rhodium mirror, and transmission relative to air. For films deposited from **1** film thicknesses were measured using the Filmetrics F20 machine operating in reflectance mode in air against an as-supplied Si standard. X-ray photoelectron spectroscopy (XPS) surface and depth profiling was performed using a Thermo Scientific K-Alpha XPS system using monochromatic Al Kα radiation at 1486.6 eV X-ray source. Etching was achieved using an Ar ion etch beam at 1 KeV with a current of 1.51 μA. CasaXPS software was used to analyses the data with binding energies referenced to an adventitious C 1s peak at 285 eV. UV/Vis/Near IR transmittance and reflectance spectra were produced using the Perkin Elmer Precisely Lambda 950 spectrometer using an air background and recorded between 320–2500 nm for films grown from **3** and **4**.

Acknowledgements

CJC and IPP thank the EPSRC for the grants EP/H00064X and EP/K001515 (CEK). SAFC Hitech are thanked for supplying $GaMe_3$. UCL is thanked for the award of an impact studentship (PJM).

References

1 P. Marchand and C. J. Carmalt, *Coord. Chem. Rev.*, 2013, **257**, 3202–3221.
2 C. E. Knapp, G. Hyett, I. P. Parkin and C. J. Carmalt, *Chem. Mater.*, 2011, **23**, 1719–1726.
3 C. E. Knapp, J. A. Manzi, A. Kafizas, I. P. Parkin and C. J. Carmalt, *ChemPlusChem*, 2014, **79**, 1024–1029.
4 L. G. Bloor, C. J. Carmalt and D. Pugh, *Coord. Chem. Rev.*, 2011, **255**, 1293–1318.
5 D. Pugh, P. Marchand, I. P. Parkin and C. J. Carmalt, *Inorg. Chem.*, 2012, **51**, 6385–6395.
6 C. Zhao, T. Witters, B. Brijs, H. Bender, O. Richard, M. Caymax, T. Heeg, J. Schubert, V. V. Afanas'ev, A. Stesmans and D. G. Schlom, *Appl. Phys. Lett.*, 2005, **86**, 132903.
7 G. D. Wilk, R. M. Wallace and J. M. Anthony, *J. Appl. Phys.*, 2001, **89**, 5243.
8 M. Kamoshida, *Appl. Phys. Lett.*, 1971, **18**, 292.
9 D. A. Mehta, S. R. Butler and F. J. Feigl, *J. Electrochem. Soc.*, 1973, **120**, 1707.
10 I. Lundström, M. Armgarth, A. Spetz and F. Winquist, *Sens. Actuators*, 1986, **10**, 399–421.
11 Chang Jin Kang, J. S. Chun and Wong Jong Lee, *Thin Solid Films*, 1990, **189**, 161–173.
12 J. A. Aboaf, *J. Electrochem. Soc.*, 1967, **114**, 948.
13 J. Saraie, *J. Electrochem. Soc.*, 1985, **132**, 890.
14 C. Carmalt and S. King, *Coord. Chem. Rev.*, 2006, **250**, 682–709.
15 M. Fleischer, S. Kornely, T. Weh, J. Frank and H. Meixner, *Sens. Actuators B Chem.*, 2000, **69**, 205–210.
16 Z. Liu, T. Yamazaki, Y. Shen, T. Kikuta, N. Nakatani and Y. Li, *Sens. Actuators B Chem.*, 2008, **129**, 666–670.
17 M. Fleischer and H. Meixner, *Sens. Actuators B Chem.*, 1991, **4**, 437–441.
18 Y. Chi, T.-Y. Chou, Y.-J. Wang, S.-F. Huang, A. J. Carty, L. Scoles, K. A. Udachin, S.-M. Peng and G.-H. Lee, *Organometallics*, 2004, **23**, 95–103.
19 S. Basharat, W. Betchley, C. J. Carmalt, S. Barnett, D. A. Tocher and H. O. Davies, *Organometallics*, 2007, **26**, 403–407.
20 C. E. Knapp, D. A. Wann, A. Bil, J. T. Schirlin, H. E. Robertson, P. F. McMillan, D. W. H. Rankin and C. J. Carmalt, *Inorg. Chem.*, 2012, **51**, 3324–3331.

21 M. Valet and D. M. Hoffman, *Chem. Mater.*, 2001, **13**, 2135–2143.
22 L. Mîinea, S. Suh, S. G. Bott, J.-R. Liu, W.-K. Chu and D. M. Hoffman, *J. Mater. Chem.*, 1999, **9**, 929–935.
23 R. Binions, C. J. Carmalt, I. P. Parkin, K. F. E. Pratt and G. A. Shaw, *Chem. Mater.*, 2004, **16**, 2489–2493.
24 O. B. Ajayi, M. S. Akanni, J. N. Lambi, C. Jeynes and J. F. Watts, *Thin Solid Films*, 1990, **185**, 123–136.
25 T. Maruyama and S. Arai, *Appl. Phys. Lett.*, 1992, **60**, 322.
26 J. S. Kim, H. A. Marzouk, P. J. Reucroft, J. D. Robertson and C. E. Hamrin, *Thin Solid Films*, 1993, **230**, 156–159.
27 J. S. Matthews, O. O. Onakoya, T. S. Ouattara and R. J. Butcher, *Dalton Trans.*, 2006, 3806.
28 C. M. Beavers, G. H. Talbo and A. F. Richards, *J. Organomet. Chem.*, 2011, **696**, 2507–2511.
29 A. Aprile, D. D. J. Wilson and A. F. Richards, *Dalton Trans.*, 2012, **41**, 8550.
30 A. F. Lugo née Gushwa and A. F. Richards, *Eur. J. Inorg. Chem.*, 2010, **2010**, 2025–2035.
31 D. J. Otway and W. S. Rees, *Coord. Chem. Rev.*, 2000, **210**, 279–328.
32 D. G. Hendershot, M. Barber, R. Kumar and J. P. Oliver, *Organometallics*, 1991, **10**, 3302–3309.
33 P. Wei, X.-W. Li and G. H. Robinson, *Chem. Commun.*, 1999, 1287–1288.
34 P. L. Gurian, L. K. Cheatham, J. W. Ziller and A. R. Barron, *J. Chem. Soc. Dalton Trans.*, 1991, 1449.
35 M. R. P. Van Vliet, P. Buysingh, G. Van Koten and K. Vrieze, *Organometallics*, 1985, **4**, 1701–1707.
36 M. North and C. Young, *Catal. Sci. Technol.*, 2011, **1**, 93.
37 A. L. Balch, R. L. Hart and S. Parkin, *Inorganica Chim. Acta*, 1993, **205**, 137–143.
38 J. Meléndez, M. North and R. Pasquale, *Eur. J. Inorg. Chem.*, 2007, **2007**, 3323–3326.
39 D. J. Darensbourg and D. R. Billodeaux, *Comptes Rendus Chim.*, 2004, **7**, 755–761.
40 P. Marchand, I. A. Hassan, I. P. Parkin and C. J. Carmalt, *Dalton Trans.*, 2013, **42**, 9406.
41 N. Bresciani-Pahor, M. Calligaris, G. Nardin, L. Randaccio and D. Viterbo, *Acta Crystallogr. B*, 1979, **35**, 2776–2778.
42 R. S. Glass, M. Sabahi, M. Hojjatie and G. S. Wilson, *Inorg. Chem.*, 1987, **26**, 2194–2196.
43 M. S. Hill and D. A. Atwood, *Eur. J. Inorg. Chem.*, 1998, **1998**, 67–72.
44 C. E. Knapp, D. Pugh, P. F. McMillan, I. P. Parkin and C. J. Carmalt, *Inorg. Chem.*, 2011, **50**, 9491–9498.
45 S. J. Dzugan and V. L. Goedken, *Inorg. Chem.*, 1986, **25**, 2858–2864.
46 D. Tian, B. Liu, Q. Gan, H. Li and D. J. Darensbourg, *ACS Catal.*, 2012, **2**, 2029–2035.
47 M.-A. Munoz-Hernandez, T. S. Keizer, P. Wei, S. Parkin and D. A. Atwood, *Inorg. Chem.*, 2001, **40**, 6782–6787.
48 H. Yu and J. W. Hutchinson, *Thin Solid Films*, 2003, **423**, 54–63.
49 C. Pflitsch, A. Muhsin, U. Bergmann and B. Atakan, *Surf. Coat. Technol.*, 2006, **201**, 73–81.
50 M. Ritala, H. Saloniemi, M. Leskelä, T. Prohaska, G. Friedbacher and M. Grasserbauer, *Thin Solid Films*, 1996, **286**, 54–58.
51 J. Sánchez-González, A. Díaz-Parralejo, A. L. Ortiz and F. Guiberteau, *Appl. Surf. Sci.*, 2006, **252**, 6013–6017.
52 S. Lars, T. Andersson and M. Scurrell, *J. Catal.*, 1979, **59**, 340–356.
53 H. E. Evans, W. M. Bowser and W. H. Weinberg, *Appl. Surf. Sci.*, 1980, **5**, 258–274.
54 A. B. Pangborn, M. A. Giardello, R. H. Grubbs, R. K. Rosen and F. J. Timmers, *Organometallics*, 1996, **15**, 1518–1520.
55 O. V. Dolomanov, L. J. Bourhis, R. J. Gildea, J. A. K. Howard and H. Puschmann, *J. Appl. Crystallogr.*, 2009, **42**, 339–341.
56 L. J. Bourhis, O. V. Dolomanov, R. J. Gildea, J. A. K. Howard and H. Puschmann, *Acta Crystallogr. Sect. Found. Adv.*, 2015, **71**, 59–75.
57 G. M. Sheldrick, *Acta Crystallogr. A*, 2008, **64**, 112–122.